Postsynaptic assembly induced by neurexin–neuroligin interaction and neurotransmitter

Christine I. Nam and Lu Chen*

Department of Molecular and Cell Biology and Helen Wills Neuroscience Institute, University of California, Berkeley, CA 94720-3200

Communicated by Roger A. Nicoll, University of California, San Francisco, CA, March 14, 2005 (received for review January 24, 2005)

Presynaptic and postsynaptic differentiation occurs at axodendritic contacts between CNS neurons. Synaptic adhesion mediated by synaptic cell adhesion molecule (SynCAM) and β-neurexins/neuroligins triggers presynaptic differentiation. The signals that trigger postsynaptic differentiation are, however, unknown. Here we report that β-neurexin expressed in nonneuronal cells induced postsynaptic density (PSD)-95 clustering in contacting dendrites of hippocampal neurons. The effect is specific to β-neurexin and was not observed with other synaptic cell adhesion molecules such as *N*-cadherin or SynCAM. NMDA receptors, but not α-amino-3-hydroxyl-5-methyl-4-isoxazolepropionate receptors (AMPARs), were recruited to this β-neurexin-induced PSD-95 scaffold. Remarkably, AMPARs were inserted into this scaffold upon glutamate application or expression of a constitutively active form of calmodulin kinase II in neurons. Expression of a dominant-negative neuroligin-1 in cultured neurons markedly reduced the sizes and densities of PSD-95 puncta and AMPAR clusters. In addition, excitatory, but not inhibitory, synaptic functions were impaired in these neurons, confirming that PSD-95/neuroligin-1 interaction is involved in postsynaptic assembly at glutamatergic synapses. These results demonstrate that postsynaptic assembly of the glutamatergic synapse may be initiated by presynaptic β-neurexin and that glutamate release also is required for maturation of synapses.

β-neurexin | glutamatergic synapse formation | synaptogenesis

Interactions between presynaptic and postsynaptic neurons are essential for synapse formation (1–5). At glutamatergic synapses in the mammalian CNS, presynaptic differentiation appears to be induced by synaptic adhesion molecules, such as synaptic cell adhesion molecule (SynCAM) and neuroligins (6–8). Mechanisms underlying CNS postsynaptic differentiation are unclear. Although major components of the postsynaptic density (PSD) have been identified, and the sequence of their assembly at nascent glutamatergic synapses has been delineated (1, 3), the axonal signals that induce postsynaptic assembly are still unknown. Recent studies indicate that β-neurexin is synaptically localized and is the axonal receptor of neuroligin-1 (NL1) (6). In addition, NL1 directly interacts with PSD-95 through its C-terminal PDZ-binding motif (9), an interaction that modulates excitatory postsynaptic formation (10–12). These findings suggest that β-neurexin/NL1 interaction may initiate postsynaptic differentiation by recruiting postsynaptic scaffolding proteins such as PSD-95.

Another potential player in postsynaptic differentiation is neurotransmitter. Observations from Munc18-1-knockout mice suggest that the initial assembly of the synapse, evaluated with ultrastructural morphology and localization of presynaptic proteins, may proceed without neurotransmitter release. However, because postsynaptic receptor localization and function were not evaluated in these mice, whether transmitter release is required for a fully functional postsynaptic assembly remains unknown (13).

Here we investigate the roles of β-neurexin and glutamate release in glutamatergic postsynaptic differentiation by using a nonneuronal cell/neuron coculture system, which allowed us to isolate and identify presynaptic signals that induce postsynaptic assembly.

Methods

For detailed information on all methods, see *Supporting Materials and Methods*, which is published as supporting information on the PNAS web site.

DNA Constructs and Antibodies. Cyan fluorescent protein (CFP)-PSD-95 was constructed by swapping CFP with GFP flanked by two *Eco*RI sites in GFP–PSD-95 construct (14). CFP-NL1-ΔC was constructed by using PCR-based mutagenesis. pHluorin–GluR1 was constructed by inserting the pHluorin-coding sequence between the third and the fourth amino acids after signal peptide cleavage site of the GluR1. Mouse SynCAM was amplified from mouse whole-brain cDNA by using the following primers: SynCAM-F, attgaattcgccaccatggcgagtgctgtgctg; and SynCAM-R, gatcgttagcggccgcctagatgaagtactctttc. pDsRed2-N1 and pIRES-DsRed2 were obtained from Clontech. Rabbit polyclonal antibody to GluR2 was from Chemicon, and mouse monoclonal antibody to PSD-95 was from Affinity BioReagents (Golden, CO).

Cell Cultures, Transfection, and Immunolabeling. Primary hippocampal cultures were prepared from the brains of rats at embryonic days 18–21 and maintained in serum-based medium with B27 supplement (Life Technologies, Carlsbad, CA). Neurons and PC12 cells were transfected by using Lipofectamine 2000 (Invitrogen). PC12 (or HEK) cells and neurons were initially cultured separately and were transfected on the same day. One day after transfection, PC12 (or HEK) cells were resuspended and plated into neuronal cultures. Confocal imaging was performed 2 days after coculturing. Immunocytochemistry was performed on cultures fixed with 2% paraformaldehyde and washed with PBS containing 0.3% Triton X-100 before incubation with primary and secondary antibodies.

Results

β-Neurexin Induces Assembly of Postsynaptic Scaffold. β-Neurexin is presynaptically expressed and interacts with postsynaptic neuroligins (6, 8). To investigate the roles of this interaction in postsynaptic assembly, we expressed β-neurexin in PC12 cells and placed them in contact with the dendrites of cultured hippocampal neurons. Because bicistronic expression of β-neurexin and DsRed (β-neurexin–internal ribosome entry site–DsRed2) does not yield high enough DsRed fluorescence for imaging purpose, in most of our experiments, we cotransfected PC12 cells with two plasmids containing β-neurexin and DsRed gene. The two-plasmid cotransfection efficiency was determined according to methods described in *Supporting Materials and Methods*. To first check whether this ectopically expressed

Abbreviations: AMPA, α-amino-3-hydroxyl-5-methyl-4-isoxazolepropionate; AMPAR, AMPA receptor; CaMKII, calmodulin kinase II; CFP, cyan fluorescent protein; EPSC, excitatory postsynaptic current; mEPSC, miniature EPSC; NL1, neuroligin-1; NMDAR, NMDA receptor; PSD, postsynaptic density; sEPSC, spontaneous EPSC; SynCAM, synaptic cell adhesion molecule.

*To whom correspondence should be addressed at: University of California, 189 LSA, Berkeley, CA 94720-3200. E-mail: luchen@uclink.berkeley.edu.

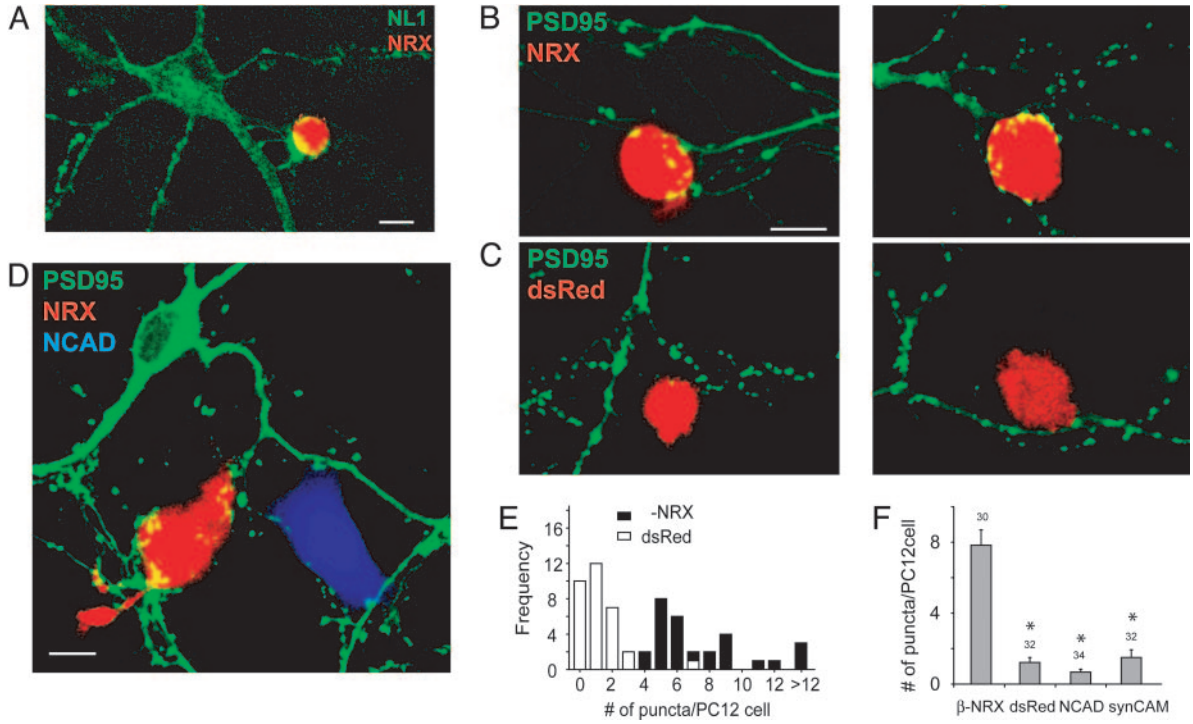

Fig. 1. β-Neurexin expressed in PC12 cells induces PSD-95 clustering in contacting dendrites of cultured hippocampal neurons. (*A*) β-Neurexin induces accumulation of NL1 in contacting dendritic regions. PC12 cells were transfected with β-neurexin and DsRed; cocultured hippocampal neurons were transfected with CFP-NL1. (*B* and *C*) β-Neurexin, but not DsRed, induces PSD-95 puncta in contacting dendritic regions. Hippocampal neurons were transfected with GFP–PSD-95 and cocultured with PC12 cells transfected with either DsRed alone or with both DsRed and β-neurexin. (*D*) *N*-cadherin does not induce PSD-95 clustering. PC12 cells transfected with either β-neurexin plus DsRed or *N*-cadherin plus CFP were cocultured with hippocampal neurons transfected with GFP–PSD-95. In a transfected neuron contacting both types of PC12 cells, strong accumulation of PSD-95 was only found in dendrites contacting the β-neurexin-expressing PC12 cell (red), but not the *N*-cadherin-expressing one (blue). (*E*) Distributions of the numbers of GFP–PSD-95 puncta next to PC12 cells expressing either β-neurexin (β-NRX; filled bar) or DsRed (open bar) (β-neurexin, $n = 30$; DsRed, $n = 32$; $P < 1 \times 10^{-10}$, single-factor ANOVA). (*F*) Average numbers of PSD-95 puncta induced by β-neurexin (β-NRX), DsRed, *N*-cadherin (NCAD), or SynCAM at contacting dendrites. (β-Neurexin, $n = 30$; DsRed, $n = 32$; *N*-cadherin, $n = 34$; SynCAM, $n = 32$; *, $P < 1 \times 10^{-5}$.)

β-neurexin is capable of binding to its postsynaptic partner NL1, we transfected neurons with CFP-tagged NL1. In these neurons, we observed robust clustering of CFP–NL1 at dendritic sites opposing transfected PC12 cells (Fig. 1*A*), suggesting that β-neurexin expressed in PC12 cells was able to recruit NL1 to the contact sites. Because PSD-95 is one of the proteins that appear early at postsynaptic site during synaptogenesis (15, 16), and NL1 interacts directly with PSD-95 (9), we wondered whether β-neurexin/NL1 interaction may initiate postsynaptic differentiation by clustering PSD-95. We examined dendritic localization of PSD-95 in hippocampal neurons contacting β-neurexin-transfected PC12 cells. GFP-tagged PSD-95 exhibited a normal, punctate distribution in cultured neurons (Fig. 1 *B–D*) (14). In addition, we observed strong punctate clustering of PSD-95 at the dendritic sites that were in contact with PC12 cells expressing β-neurexin (Fig. 1 *B* and *D*). When dendrites came into contact with these PC12 cells, they sent out a large number of spine-like contacts "grabbing" onto the PC12 cells. DsRed-expressing PC12 cells does not induce such morphologically unique clustering of GFP–PSD-95 (Fig. 1*C*). Strong PSD-95 accumulation in contacting dendrites was found for all of the 30 β-neurexin-expressing PC12 cells examined (Fig. 1*E*). In contrast, of the 32 DsRed-expressing PC12 cells that had dendrites crossing through, 11 did not have any GFP–PSD-95 puncta in the contacting dendritic regions (Fig. 1*E*). On average, each β-neurexin-expressing PC12 cell induced 7.83 ± 0.87 PSD-95 puncta in the contacting dendritic regions, whereas 1.22 ± 0.25 puncta were detected in dendritic regions touching each DsRed-expressing PC12 cell (Fig. 1*F*).

We examined whether other synaptic adhesion molecules can also induce PSD-95 accumulation. We transfected two separate dishes of PC12 cells with either β-neurexin (coexpressing DsRed) or *N*-cadherin (coexpressing CFP) and plated these two groups of PC12 cells together on top of cultured hippocampal neurons transfected with GFP–PSD-95. When dendrites from the same neuron contacted both β-neurexin-expressing (red) and *N*-cadherin-expressing (blue) PC12 cells, strong GFP–PSD-95 clustering was only found at the sites next to the β-neurexin-expressing, but not the *N*-cadherin-expressing, PC12 cells (Fig. 1*D*). Of the 34 *N*-cadherin-expressing PC12 cells that had dendrites crossing through, 18 cells did not have any PSD-95 puncta in the contacting dendritic regions. On average, 0.68 ± 0.16 puncta were detected in dendritic regions touching each *N*-cadherin-expressing PC12 cell. SynCAM, another homophilic synaptic adhesion molecule that is able to induce presynaptic differentiation (7) and increase excitatory synaptic responses when overexpressed (10), also failed to induce accumulation of PSD-95 in contacting dendrites (1.75 ± 0.28 puncta per cell; Fig. 1*E*). Thus, the PSD-95 clustering effect we observed was specific for β-neurexin.

We observed a small number of PSD-95 puncta in the dendrites that contacted with some PC12 cells expressing DsRed alone, *N*-cadherin, or SynCAM (Fig. 1 *C* and *D*). These PSD-95 puncta did not show the unique grabbing morphology and presumably represent synaptic sites formed between the dendrites of the transfected neuron and axons of neighboring untransfected neurons. To confirm that most of the PSD-95 puncta found on dendritic regions contacting β-neurexin-expressing PC12 cells were indeed induced by β-neurexin and were not associated with synaptic boutons, we

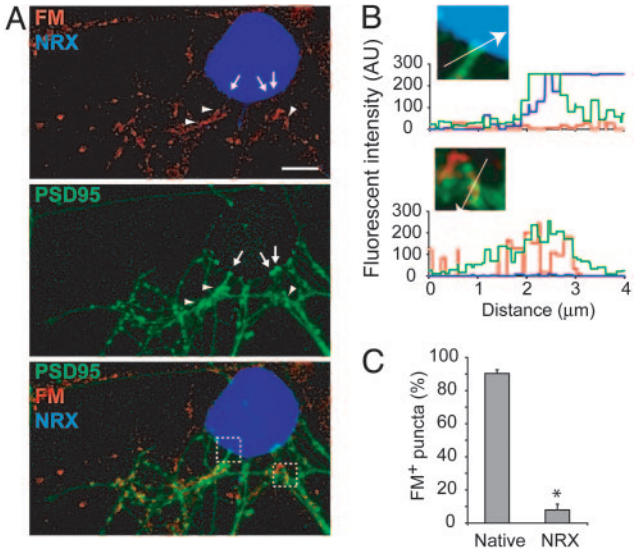

Fig. 2. Lack of presynaptic transmitter release sites associated with β-neurexin-induced PSD-95 puncta. (*A*) The synaptic GFP–PSD-95 clusters colocalized with functional presynaptic terminals identified by FM 4-64 staining (arrowheads), whereas PSD-95 puncta formed on the PC12 cell (coexpressing CFP with β-neurexin) lacked functional presynaptic release sites (arrows). (Scale bar, 10 μm.) (*B*) Fluorescence intensity profiles across two GFP–PSD-95 puncta (white boxes in *A*). One was formed on the PC12 cell; the other was synaptic. (*C*) Percentage overlap of GFP–PSD-95 puncta with FM 4-64 staining at native and β-neurexin-induced sites. ($n = 12$ cell pairs; ⋆, $P < 1 \times 10^{-10}$.)

performed FM 4-64 staining to visualize all functional presynaptic release sites. Most native PSD-95 puncta were juxtaposed to presynaptic release sites (90.4 ± 2.2%), indicating that they were synaptic. By contrast, very little FM 4-64 labeling was detected next to the PSD-95 puncta contacting neurexin-transfected PC12 cells (7.9 ± 4.4%) (Fig. 2).

NMDA Receptors (NMDARs), but Not α-Amino-3-hydroxyl-5-methyl-4-isoxazolepropionate Receptors (AMPARs), Are Present in β-Neurexin-Induced Postsynaptic Scaffold. Functional postsynaptic structure is signified by the presence of neurotransmitter receptors. We next examined whether β-neurexin induces postsynaptic receptor clustering. We transfected hippocampal neurons with both CFP–PSD-95 and GFP-GluR1. The two-plasmid coexpression efficiency in neurons was evidently high, indicated by the presence of both GFP and CFP signals in all transfected neurons examined. In a few transfected neurons, we photobleached one fluorophore and found that the intensity of the other fluorophore was not affected, indicating that the bleed-through between CFP and GFP channels was minimal under the imaging settings we used for these experiments. In the transfected neurons cocultured with β-neurexin-expressing PC12 cells, CFP–PSD-95 puncta were observed at the sites of contact (Fig. 3*A*). However, only 20.56 ± 5.10% of the PSD-95 puncta formed on PC12 cells contained GFP-GluR1 clusters, which was much lower than the percentage of overlap for nearby PSD-95 puncta on the same dendrites (67.00 ± 2.01%; Fig. 3*B*). We also expressed GFP-NR2A and CFP–PSD-95 in neurons and examined NMDARs clustering around β-neurexin-expressing PC12 cells. The percentages of PSD-95 puncta that contained NMDARs were similar between the native and β-neurexin-induced sites (native, 58.97 ± 3.95%; β-neurexin, 59.32 ± 4.93%; Fig. 3 *C* and *D*). The incomplete overlap of PSD-95 with NMDA and AMPARs at synapses agrees with observations made from immunocytochemistry in young cultured hippocampal neurons (15).

To confirm our observations, we examined endogenously expressed synaptic proteins. We plated HEK 293 cells coexpressing β-neurexin and DsRed into hippocampal neuronal cultures. Endogenous PSD-95 immunofluorescence accumulated strongly around these HEK 293 cells (see Fig. 7*A*, which is published as supporting information on the PNAS web site). The same phenomenon was not observed if HEK cells were expressing DsRed only (Fig. 7*B*). The clustering of PSD-95 immunofluorescence around β-neurexin-expressing HEK cells appeared more dramatic than those observed with exogenously expressed GFP–PSD-95 (Fig. 1*B*), possibly because immunostaining revealed PSD-95 in all contacting dendrites from many nearby neurons, whereas GFP–PSD-95 signals only reflected the clustering of PSD-95 in the transfected neuron. The PSD-95 signals around β-neurexin-expressing HEK cells were so strong that it was not always possible to separately visualize individual puncta. We therefore quantified the total number of PSD-95-positive pixels instead of the number of puncta. On average, 2,935.6 ± 663.8 PSD-95-positive pixels were found to colocalize with each β-neurexin-expressing HEK cell, and this number was reduced to 388.2 ± 97.0 when HEK cells expressed DsRed only ($n = 10$

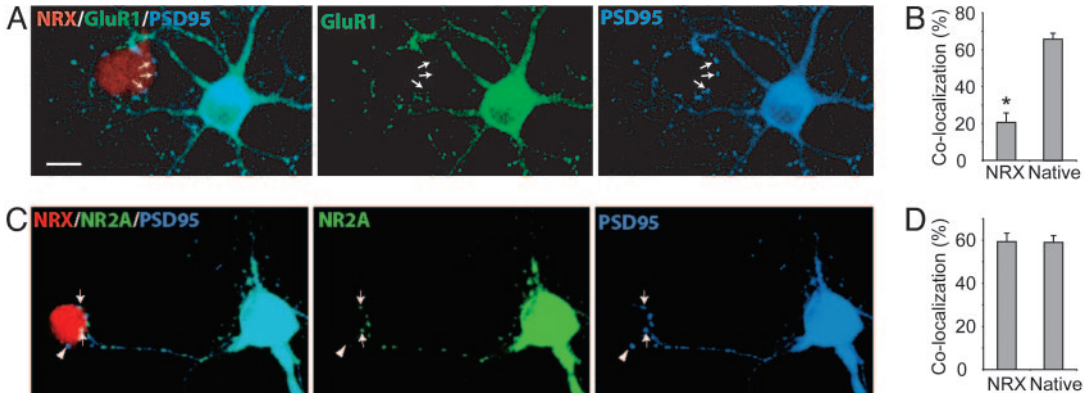

Fig. 3. NMDARs, but not AMPARs, are present in β-neurexin-induced PSD-95 puncta. (*A*) The lack of AMPARs in β-neurexin-induced PSD-95 puncta. Neurons were transfected with CFP–PSD-95 and GFP-GluR1. Cocultured PC12 cells were transfected with β-neurexin and DsRed. *Z*-stack images from multiple focal planes were examined. Although PSD-95 formed clusters around PC12 cells, most of these clusters did not contain AMPARs (arrows). (*B*) Percentages of GluR1-positive β-neurexin-induced (NRX) and neighboring PSD-95 (Native) puncta ($n = 26$ cell pairs; ⋆, $P < 1 \times 10^{-5}$). (*C*) The presence of NMDARs in β-neurexin-induced PSD-95 puncta. Neurons were transfected with CFP–PSD-95 and GFP-NR2A. Cocultured PC12 cells were transfected with β-neurexin and DsRed. Although most of the PSD-95 puncta induced by β-neurexin contained NMDAR (arrows), a small percentage of them did not (arrowheads). (*D*) The percentage of NR2A-positive synaptic PSD-95 puncta (Native) is similar to that of the β-neurexin-induced (NRX) ones ($n = 20$ cell pairs; $P > 0.5$). (Scale bar, 10 μm.)

for each group; $P < 1 \times 10^{-5}$). Similar to what we have observed with exogenously expressed GFP-GluR1, endogenous AMPAR immunofluorescence was not elevated around β-neurexin-expressing HEK cells (Fig. 7*C*, $n = 12$), indicating that the PSD-95 clusters formed around β-neurexin-expressing cells lacked AMPARs.

Calmodulin Kinase II (CaMKII) Activity or NMDAR Activation Drives AMPARs into β-Neurexin-Induced Postsynaptic Structure. The presence of NMDARs, but not AMPARs, in β-neurexin-induced PSD-95 puncta is reminiscent of "silent synapses" that normally occur during synapse development. CaMKII activation has been shown to turn on silent synapses through a long-term potentiation-like process (17, 18). We therefore examined whether activation of CaMKII can also drive AMPARs into the β-neurexin-induced structure. Expression of a truncated, constitutively active CaMKII increased colocalization of GluR1 with β-neurexin-induced PSD-95 puncta to 83.87 ± 8.57% (Fig. 4*A*; $n = 16$). The colocalization of PSD-95 and GluR1 puncta on neighboring dendrites was also increased from 67.00 ± 2.01% to 88.03 ± 5.13% ($n = 16$), possibly due to the activation of native silent synapses.

NMDAR activation leads to rapid synaptic insertion of AMPARs (19), a process that is involved in activation of the silent synapse and in certain types of long-term potentiation. To test whether a similar process may occur in the β-neurexin-induced structure, we examined membrane insertion of AMPARs after glutamate application. We generated an N-terminal-tagged pHluorin (Ecliptic pH-sensitive GFP)-GluR1 to monitor receptor insertion. Fluorescent signal of pHluorin increased significantly when pH changed from acidic (<6.0) to neutral (7.0–8.0). Because the pH inside most intracellular trafficking vesicles is slightly acidic, an increase in pHluorin fluorescence indicates vesicle exocytosis and plasma membrane insertion of the tagged proteins (20). We first examined the localization of pHluorin-GluR1 in hippocampal neurons coexpressing CFP–PSD-95 with pHluorin-GluR1. Both the dendritic spines and shaft of the neurons had pHluorin-GluR1 signals. The bright punctated pHluorin-GluR1 signals appeared to be in the spines and were colocalized with CFP–PSD-95 (Fig. 4*B*). When the external solution pH was changed to 6, pHluorin-GluR1 signals in spines were completely diminished, and the shaft signals were reduced. In contrast, CFP–PSD-95 signal was not affected by the pH change (Fig. 4*B*). This result suggests that bright pHluorin-GluR1 puncta indeed represent the surface AMPAR clusters. We next plated β-neurexin-expressing PC12 cells onto these double-transfected neurons. After 2 days of coculturing, we activated NMDARs of the cultured neurons with glutamate (100 μM) and glycine (40 μM). Cyclothiazide (50 μM) also was included to block AMPAR desensitization and promote removal of magnesium blockade of NMDARs. Glutamate and glycine were bath-applied in brief pulses (10 pulses with a 10-sec pulse duration and a 30-sec interpulse interval). Small bath volume was used (400 μl) to ensure fast and complete solution exchange because brief activation of NMDARs induces synaptic AMPAR insertion, whereas their prolonged activation causes AMPAR internalization (21, 22). *Z*-stack images from all focal planes were taken for each time point to avoid any artifacts that may occur because of focal plane shift. Because an increase in pHluorin-GluR1 fluorescence indicates membrane insertion of the AMPARs as suggested by results from Fig. 4*B*, we looked for appearance of pHluorin-GluR1 signals in dendrites contacting β-neurexin-expressing PC12 cells. Ten of the 12 neuron-PC12 cell pairs that were examined had appearance of pHluorin-GluR1 signals after 10–20 min of glutamate application at sites where only CFP–PSD-95 puncta had been detected before (Fig. 4*C*). These results indicate that the β-neurexin-induced PSD-95 scaffold is not merely an aggregation of proteins but is functional for supporting AMPAR insertion upon NMDAR activation.

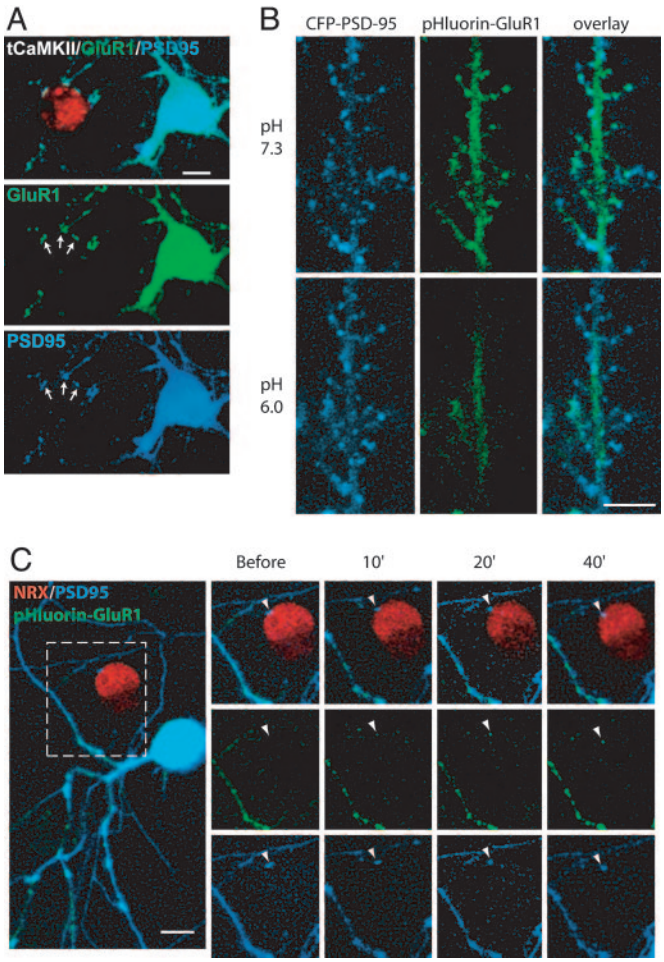

Fig. 4. Activation of CaMKII or NMDARs drives AMPARs into β-neurexin-induced PSD-95 puncta. (*A*) Insertion of GluR1 into β-neurexin-induced PSD-95 puncta by CaMKII activity. Hippocampal neurons were cotransfected with truncated constitutively active CaMKII (tCaMKII), GFP-GluR1, and CFP-PSD-95 and cocultured with PC12 cells expressing β-neurexin and DsRed. Most of the β-neurexin-induced PSD-95 puncta have GluR1 clusters (arrows). (*B*) pHluorin-GluR1 signal as an indicator for surface-expressed AMPARs. Hippocampal neurons were cotransfected with CFP–PSD-95 and pHluorin-GluR1. At pH 7.3, pHluorin-GluR1 puncta were visible in spines and colocalized with PSD-95, indicative of their synaptic localization. When the external solution pH was changed to 6.0, all of the pHluorin-GluR1 signal in spines disappeared, indicating that most of the pHluorin puncta represented surface AMPARs. (*C*) Insertion of pHluorin-GluR1 into β-neurexin-induced PSD-95 puncta by glutamate. Glutamate and glycine were bath-applied in brief pulses. pHluorin-GluR1 signal appears 10–20 min after the application and remains for at least another 20 min (arrowheads). (All scale bars, 10 μm.)

Expression of NL1 Mutant Reduces Clustering of Synaptic Proteins. The results we obtained so far suggest that exogenous β-neurexin may induce the postsynaptic assembly. We next examined whether β-neurexin/NL1 interaction plays a role in postsynaptic differentiation during normal synapse formation in neurons. Because β-neurexin/NL1 interaction is also important for presynaptic differentiation (8), we generated a mutant NL1 construct, NL1–ΔC, to selectively target postsynaptic protein interaction. This NL1–ΔC lacks the last four amino acids in the C terminus required for its binding to PSD-95 (9), thus acting as a dominant-negative when expressed in neurons to disrupt β-neurexin-induced PSD-95 clustering. We expressed GFP either alone

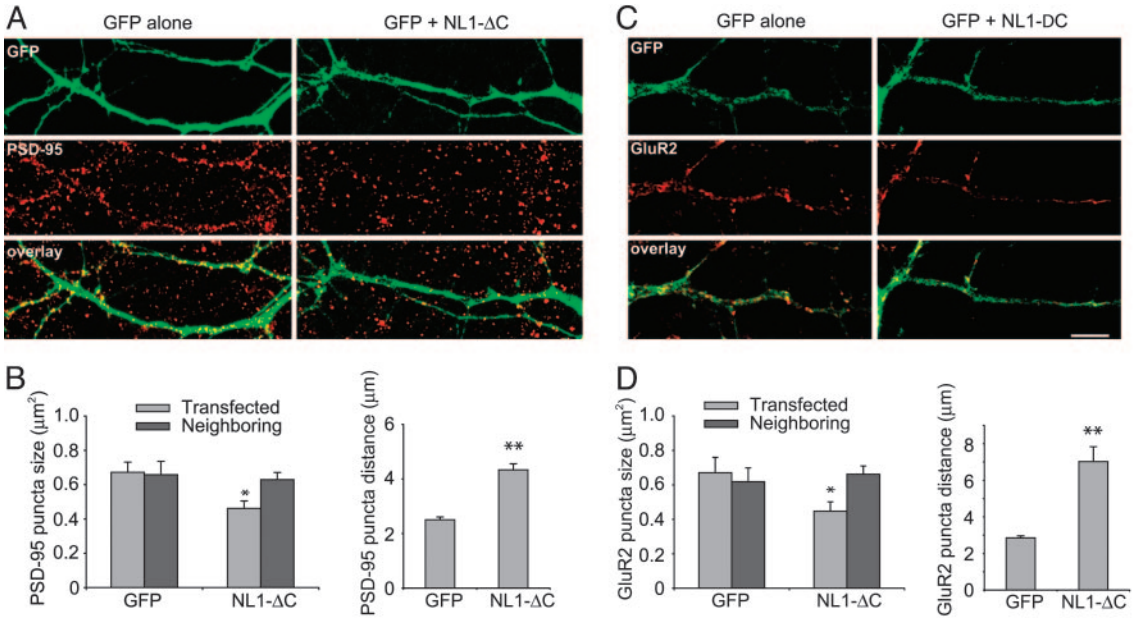

Fig. 5. NL1-ΔC reduces synaptic clustering of PSD-95 and glutamate receptors. (*A* and *B*) Reduced PSD-95 immunofluorescence in NL1-ΔC-expressing neurons. Hippocampal neurons were transfected with GFP alone or GFP plus NL1-ΔC and stained for PSD-95. NL1-ΔC expression significantly reduced PSD-95 puncta size and density (GFP, $n = 595$; untransfected GFP neighboring, $n = 314$; NL1-ΔC, $n = 532$; untransfected NL1-ΔC neighboring, $n = 902$; *, $P < 0.01$; **, $P < 0.001$). (*C* and *D*) Reduced GluR2 puncta in NL1-ΔC-expressing neurons (GFP, $n = 667$; untransfected GFP neighboring, $n = 472$; NL1-ΔC, $n = 548$; untransfected NL1-ΔC neighboring, $n = 631$; *, $P < 0.005$; **, $P < 0.001$). (Scale bar, 10 μm.)

or together with CFP–NL1–ΔC in hippocampal neurons. GFP was expressed in both groups and was used to help determine contours of the transfected neurons. CFP signal was always monitored for each cell to ensure that CFP–NL1–ΔC was expressed. Hippocampal cultures were transfected on days 8 or 9 days *in vitro*, and examined on days 10–12 days *in vitro*, encompassing a period of rapid synaptogenesis. PSD-95 immunofluorescence in neurons transfected with NL1–ΔC was reduced compared with that in neighboring untransfected neurons or GFP-transfected neurons on sister cover slips (Fig. 5 *A* and *B*). Both PSD-95 puncta size and density were significantly reduced in NL1–ΔC-expressing neurons (size: GFP, 0.67 ± 0.03 μm^2; untransfected GFP-neighboring, 0.65 ± 0.03 μm^2; NL1–ΔC, 0.46 ± 0.02 μm^2; untransfected NL1–ΔC-neighboring, 0.63 ± 0.02 μm^2; puncta distance: GFP, 2.51 ± 0.07 μm; NL1–ΔC, 4.34 ± 0.14 μm). In addition, AMPAR clustering was impaired in NL1–ΔC-transfected neurons indicated by reduced GluR2 immunofluorescence (size: GFP, 0.67 ± 0.09 μm^2; untransfected GFP-neighboring, 0.62 ± 0.08 μm^2; NL1–ΔC, 0.45 ± 0.05 μm^2; untransfected NL1–ΔC-neighboring, 0.66 ± 0.05 μm^2; puncta distance: GFP, 2.86 ± 0.11 μm; NL1–ΔC, 7.03 ± 0.81 μm) (Fig. 5 *C* and *D*).

Excitatory, but Not Inhibitory, Synaptic Transmission Is Impaired in Neurons Expressing NL1 Mutant. We next examined excitatory postsynaptic currents (EPSCs) and inhibitory postsynaptic currents in NL1-ΔC-transfected neurons. AMPAR-mediated miniature EPSCs (mEPSCs) were markedly reduced in NL1-ΔC-transfected neurons in both amplitude (control, 20.10 ± 1.31 pA; NL1–ΔC, 12.21 ± 0.70 pA) and frequency (control, 6.27 ± 1.10 Hz; NL1-ΔC, 1.83 ± 1.10 Hz) (see Fig. 6 *A* and *C*). To assess synaptic NMDAR functions, we measured action potential-driven NMDA spontaneous EPSCs (sEPSCs) instead of estimating the NMDA mEPSC component by using dual-component mEPSCs, because the reduced α-amino-3-hydroxyl-5-methyl-4-isoxazolepropionate (AMPA) mEPSCs may cause underestimation of the NMDA mEPSC component in NL1–ΔC-transfected cells. The amplitude of NMDA sEPSCs was significantly reduced (control, 564.10 ± 70.10 pA; NL1–ΔC, 318.25 ± 55.92 pA) by NL1–ΔC expression (Fig. 6 *B* and *D*). The frequencies of NMDA sEPSCs were not different between untransfected and NL1–ΔC-transfected cells (control,

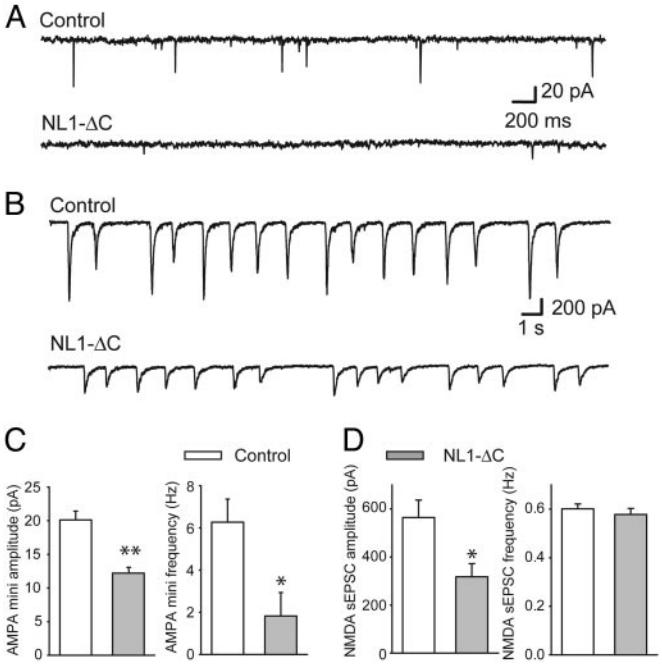

Fig. 6. NL1-ΔC selectively down-regulates excitatory synaptic functions. (*A*) AMPA mEPSC traces from NL1-ΔC-expressing and neighboring untransfected (control) neurons. (*B*) NMDA sEPSC traces. (*C*) NL1-ΔC expression down-regulates AMPA mEPSC amplitude and frequency (control, $n = 17$; NL1-ΔC, $n = 15$; *, $P < 0.01$; **, $P < 1 \times 10^{-4}$). (*D*) NL1-ΔC transfection reduces synaptic NMDA sEPSC amplitude without affecting presynaptic firing frequency (control, $n = 16$; NL1-ΔC, $n = 15$; *, $P < 0.01$).

0.60 ± 0.02 Hz; NL1–ΔC, 0.58 ± 0.03 Hz), indicating that the spontaneous firing frequencies of the untransfected presynaptic cells were not different. In contrast to the impaired excitatory synaptic transmission, inhibitory synaptic functions were not significantly altered in NL1–ΔC-transfected cells (miniature inhibitory postsynaptic current amplitude: control, 23.65 ± 1.67 pA; NL1–ΔC, 28.13 ± 4.58 pA; $P > 0.1$; frequency: control, 1.84 ± 0.37 Hz; NL1–ΔC, 1.15 ± 0.26 Hz; $P > 0.1$).

Discussion

In the present study, we demonstrated that a single presynaptic molecule, β-neurexin, could induce a postsynaptic scaffold structure. Remarkably, this scaffold functions like the postsynaptic silent synapse: when activated by neurotransmitter, it recruits AMPARs. The parallels between β-neurexin-induced postsynaptic differentiation and natural synaptogenesis (15, 16) suggest that they share similar mechanisms. Our findings also reveal a link between axodendritic contact and initiation of postsynaptic differentiation. β-neurexin/NL1 interaction not only provides an instructive signal determining the site of postsynaptic protein assembly but also triggers the first step of this process: the formation of postsynaptic scaffold.

The colocalization of NMDAR clusters with some β-neurexin-induced PSD-95 puncta is an interesting observation. Although PSD-95 directly binds to NR2 subunits (23, 24), its role in synaptic NMDAR clustering is unclear. The C-terminal region of the NMDAR subunit, which interacts with PDZ proteins, is required for its synaptic localization (25, 26). However, NR-1 is not present at all PSD-95 clusters in young hippocampal culture (15), and manipulating the synaptic PSD-95 level does not seem to affect synaptic NMDAR quantity or functions (27–29). We observed similar distribution patterns for both native and β-neurexin-induced PSD-95 and NR2A clusters; NMDARs are present at some but not all PSD-95 clusters. It is possible that other membrane-associated guanylate kinase family members, such as PSD-93 or SAP-102 (30, 31), mediate neurexin-induced and normal synaptic clustering of NMDARs.

The interaction between β-neurexin and NL1 initiates postsynaptic assembly, but the induced structure lacks AMPARs, mimicking the silent synapse often observed during synapse development (32). The transformation of silent to functional synapses is mediated by long-term potentiation-like mechanisms that involve NMDAR activation and CaMKII activity (33). We were able to induce AMPAR insertion into the β-neurexin-induced structure with CaMKII activation or glutamate stimulation, suggesting that the induced structure contains sufficient postsynaptic machinery to support such transformation. It also suggests that postsynaptic differentiation is a multistep process that requires more than just synaptic adhesion. The formation of the postsynaptic scaffold is probably a hard-wired first step that mainly relies on direct protein interactions at the sites of presynaptic contact and postsynaptic NL1 clustering. The second step, the turning on of the silent synapse, requires presynaptic release of glutamate, a process that also can be triggered by transsynaptic interaction of adhesion molecules (7, 8). Finally, functional synapses are maintained and adjusted under the instructions of patterned network activity.

In addition to β-neurexin and NL1, other synaptic adhesion molecules have also been suggested to play roles in synapse formation, such as SynCAM and Ephrin-Eph receptors (7, 10, 34). Different types of synaptic adhesion molecules may work in parallel to initiate synapse formation. It is also possible that the initiation of postsynaptic differentiation is mediated by β-neurexin–NL1 interaction, and maturation and stabilization of the postsynaptic structure require other types of adhesion molecules. In any case, concurrent presynaptic and postsynaptic differentiation can be triggered by the same pair of adhesion molecules, which provides a simple way of aligning presynaptic and postsynaptic compartments.

We thank Peter Scheiffele (Columbia University, New York) for providing β-neurexin and NL1 cDNAs; Ehud Isacoff (University of California, Berkeley) for providing CFP-NL1; David Bredt (Eli Lilly) for providing GFP–PSD-95; Roger Nicoll (University of California, San Francisco) for providing GFP-GluR1 and tCaMKII; Stefano Vicini (Georgetown University Medical Center, Washington, DC) for providing GFP-NR2A; and Joshua Kaplan (Massachusetts General Hospital, Boston) for providing pHluorin. This work was supported by grants from the Mabel and Arnold Beckman Foundation and the David and Lucile Packard Foundation (to L.C.).

1. Garner, C. C., Zhai, R. G., Gundelfinger, E. D. & Ziv, N. E. (2002) *Trends Neurosci.* **25,** 243–251.
2. Jin, Y. (2002) *Curr. Opin. Neurobiol.* **12,** 71–79.
3. Li, Z. & Sheng, M. (2003) *Nat. Rev. Mol. Cell Biol.* **4,** 833–841.
4. Sanes, J. R. & Lichtman, J. W. (2001) *Nat. Rev. Neurosci.* **2,** 791–805.
5. Ziv, N. E. & Garner, C. C. (2004) *Nat. Rev. Neurosci.* **5,** 385–399.
6. Dean, C., Scholl, F. G., Choih, J., DeMaria, S., Berger, J., Isacoff, E. & Scheiffele, P. (2003) *Nat. Neurosci.* **6,** 708–716.
7. Biederer, T., Sara, Y., Mozhayeva, M., Atasoy, D., Liu, X., Kavalali, E. T. & Sudhof, T. C. (2002) *Science* **297,** 1525–1531.
8. Scheiffele, P., Fan, J., Choih, J., Fetter, R. & Serafini, T. (2000) *Cell* **101,** 657–669.
9. Irie, M., Hata, Y., Takeuchi, M., Ichtchenko, K., Toyoda, A., Hirao, K., Takai, Y., Rosahl, T. W. & Sudhof, T. C. (1997) *Science* **277,** 1511–1515.
10. Sara, Y., Biederer, T., Atasoy, D., Chubykin, A., Mozhayeva, M. G., Sudhof, T. C. & Kavalali, E. T. (2005) *J. Neurosci.* **25,** 260–270.
11. Prange, O., Wong, T. P., Gerrow, K., Wang, Y. T. & El-Husseini, A. (2004) *Proc. Natl. Acad. Sci. USA* **101,** 13915–13920.
12. Graf, E. R., Zhang, X., Jin, S. X., Linhoff, M. W. & Craig, A. M. (2004) *Cell* **119,** 1013–1026.
13. Verhage, M., Maia, A. S., Plomp, J. J., Brussaard, A. B., Heeroma, J. H., Vermeer, H., Toonen, R. F., Hammer, R. E., van den Berg, T. K., Missler, M., *et al.* (2000) *Science* **287,** 864–869.
14. Craven, S. E., El-Husseini, A. E. & Bredt, D. S. (1999) *Neuron* **22,** 497–509.
15. Rao, A., Kim, E., Sheng, M. & Craig, A. M. (1998) *J. Neurosci.* **18,** 1217–1229.
16. Friedman, H. V., Bresler, T., Garner, C. C. & Ziv, N. E. (2000) *Neuron* **27,** 57–69.
17. Wu, G., Malinow, R. & Cline, H. T. (1996) *Science* **274,** 972–976.
18. Poncer, J. C., Esteban, J. A. & Malinow, R. (2002) *J. Neurosci.* **22,** 4406–4411.
19. Shi, S. H., Hayashi, Y., Petralia, R. S., Zaman, S. H., Wenthold, R. J., Svoboda, K. & Malinow, R. (1999) *Science* **284,** 1811–1816.
20. Miesenbock, G., De Angelis, D. A. & Rothman, J. E. (1998) *Nature* **394,** 192–195.
21. Beattie, E. C., Carroll, R. C., Yu, X., Morishita, W., Yasuda, H., von Zastrow, M. & Malenka, R. C. (2000) *Nat. Neurosci.* **3,** 1291–1300.
22. Lu, W., Man, H., Ju, W., Trimble, W. S., MacDonald, J. F. & Wang, Y. T. (2001) *Neuron* **29,** 243–254.
23. Kornau, H. C., Schenker, L. T., Kennedy, M. B. & Seeburg, P. H. (1995) *Science* **269,** 1737–1740.
24. Niethammer, M., Kim, E. & Sheng, M. (1996) *J. Neurosci.* **16,** 2157–2163.
25. Mori, H., Manabe, T., Watanabe, M., Satoh, Y., Suzuki, N., Toki, S., Nakamura, K., Yagi, T., Kushiya, E., Takahashi, T., *et al.* (1998) *Neuron* **21,** 571–580.
26. Steigerwald, F., Schulz, T. W., Schenker, L. T., Kennedy, M. B., Seeburg, P. H. & Kohr, G. (2000) *J. Neurosci.* **20,** 4573–4581.
27. Migaud, M., Charlesworth, P., Dempster, M., Webster, L. C., Watabe, A. M., Makhinson, M., He, Y., Ramsay, M. F., Morris, R. G., Morrison, J. H., *et al.* (1998) *Nature* **396,** 433–439.
28. El-Husseini, A. E., Schnell, E., Chetkovich, D. M., Nicoll, R. A. & Bredt, D. S. (2000) *Science* **290,** 1364–1368.
29. El-Husseini Ael, D., Schnell, E., Dakoji, S., Sweeney, N., Zhou, Q., Prange, O., Gauthier-Campbell, C., Aguilera-Moreno, A., Nicoll, R. A. & Bredt, D. S. (2002) *Cell* **108,** 849–863.
30. Tao, Y. X., Rumbaugh, G., Wang, G. D., Petralia, R. S., Zhao, C., Kauer, F. W., Tao, F., Zhuo, M., Wenthold, R. J., Raja, S. N., *et al.* (2003) *J. Neurosci.* **23,** 6703–6712.
31. Sans, N., Prybylowski, K., Petralia, R. S., Chang, K., Wang, Y. X., Racca, C., Vicini, S. & Wenthold, R. J. (2003) *Nat. Cell Biol.* **5,** 520–530.
32. Isaac, J. T. (2003) *Neuropharmacology* **45,** 450–460.
33. Nicoll, R. A. (2003) *Philos. Trans. R. Soc. London B* **358,** 721–726.
34. Dalva, M. B., Takasu, M. A., Lin, M. Z., Shamah, S. M., Hu, L., Gale, N. W. & Greenberg, M. E. (2000) *Cell* **103,** 945–956.